Semiconductor Physics, Quantum Electronics & Optoelectronics, 2008. V. 11, N 2. P. 171-177.

PACS 77.80.Fm, 77.65.-j, 68.37.-d

The resolution function and effective response of piezoelectric thin films in Piezoresponse Force Microscopy

A.N. Morozovska
V. Lashkaryov Institute of Semiconductor Physics, National Academy of Science of Ukraine,
45, prospect Nauky, 03028 Kyiv, Ukraine; e-mail: morozo@i.com.ua

Abstract. The elastic Green function and resolution function in Piezoresponse Force Microscopy (PFM) of thin piezoelectric film capped on the rigid substrate are derived. The extrinsic size effect on the resolution function is demonstrated.

Keywords: Piezoresponse Force Microscopy, thin piezoelectric films, resolution function.

Manuscript received 28.09.07; accepted for publication 10.04.08; published online 30.07.08.

1. Introduction

Verification of existing theoretical models, design of functional nanomaterials with predetermined properties, and application in various devices necessitate experimental and theoretical studies of piezoelectric coupling and ferroelectric properties in surface layers. These considerations of the local polarization switching behavior in thin films are possible in the context of Piezoresponse Force Microscopy (PFM) [1, 2].

Conventional framework for the PFM data analysis was based on the 1D models suggested originally by Ganpule, thus ignoring the 3D geometry of the PFM problem. Only recently, the decoupled theory [3, 4] was applied to derive analytical expressions for PFM response on semi-infinite materials of low symmetry, derive analytical expressions for resolution function and domain wall profiles, and interpret PFM spectroscopy data [5].

Further, the local piezoresponse dependence on film thickness was predicted in [6] for thin films capped on the nonpiezoelectric bulk with the same elastic and close dielectric properties. In the paper, the complementary case of thin piezoelectric films capped on rigid substrates is considered within the framework of decoupled approximation. For ferroelectric perovskite films like $BaTiO_3$ or $Pb(Ti, Zr)O_3$ rigid dielectric substrates are MgO oxide, sapphire Al_2O_3 or carbon with effective dielectric constant $\kappa_b \approx 5-10$. Silicon ($\kappa_b \approx 3-12$) and SiO_2 ($\kappa_b \approx 5$) have smaller elastic stiffness than typical perovskites.

2. Elastic Green function of thin film on rigid substrate

Let us derive the elastic Green function for the layer on the rigid substrate. General equation for the field of elastic displacement vector is [7]:

$$\Delta_{\mathbf{x}}\mathbf{u} + \frac{1}{1-2\nu}\,\mathrm{grad}_{\mathbf{x}}(\mathrm{div}_{\mathbf{x}}\mathbf{u}) = -\frac{2(1+\nu)}{Y}\boldsymbol{F}\cdot\delta(\mathbf{x}-\boldsymbol{\xi})\,. \tag{1a}$$

Here the vector $\mathbf{x}$ denotes the given location and $\boldsymbol{\xi}$ is the point at which the point force, $\boldsymbol{F}$, is applied. The material is isotropic and ν is the Poisson coefficient, Y is the Young modulus. Introducing the shear modulus $\mu = Y/(2(1+\nu))$, Eq. (1a) can be rewritten as:

$$\frac{\partial^2 u_i}{\partial x_k \partial x_k} + \frac{1}{1-2\nu}\frac{\partial^2 u_m}{\partial x_i \partial x_m} = -\frac{F_i}{\mu}\delta(\mathbf{x}-\boldsymbol{\xi})\,. \tag{1b}$$

Introducing transversal Fourier transformation

$$\widetilde{u}_i(k_1,k_2,x_3) = \frac{1}{2\pi}\int_{-\infty}^{\infty}dx_1\int_{-\infty}^{\infty}dx_2\,\exp(ik_1x_1+ik_2x_2)\cdot u_i(\mathbf{x})\,, \tag{2a}$$

$$u_i(\mathbf{x}) = \frac{1}{2\pi}\int_{-\infty}^{\infty}dk_1\int_{-\infty}^{\infty}dk_2\,\exp(-ik_1x_1-ik_2x_2)\,\widetilde{u}_i(k_1,k_2,x_3), \tag{2b}$$

and using integral representation of the delta function

$$\delta(x_1-\xi_1)\delta(x_2-\xi_2)= \\ =\frac{1}{(2\pi)^2}\int\limits_{-\infty}^{\infty}\int\limits_{-\infty}^{\infty}dk_1dk_2\exp\bigl(-ik_1(x_1-\xi_1)-ik_2(x_2-\xi_2)\bigr). \tag{3}$$

Eq. (1b) yields:

$$\begin{cases} -\bigl(k_1^2(1+\alpha)+k_2^2\bigr)\widetilde{u}_1+\dfrac{\partial^2\widetilde{u}_1}{\partial x_3^2}-\alpha k_1k_2\widetilde{u}_2-i\alpha k_1\dfrac{\partial\widetilde{u}_3}{\partial x_3}= \\ -\dfrac{F_1}{2\pi\mu}\exp\bigl(ik_1\xi_1+ik_2\xi_2\bigr)\delta(x_3-\xi_3) \\ -\alpha k_1k_2\widetilde{u}_1-\bigl(k_1^2+k_2^2(1+\alpha)\bigr)\widetilde{u}_2+\dfrac{\partial^2\widetilde{u}_2}{\partial x_3^2}-i\alpha k_2\dfrac{\partial\widetilde{u}_3}{\partial x_3}= \\ -\dfrac{F_2}{2\pi\mu}\exp\bigl(ik_1\xi_1+ik_2\xi_2\bigr)\delta(x_3-\xi_3) \\ -i\alpha k_1\dfrac{\partial\widetilde{u}_1}{\partial x_3}-i\alpha k_2\dfrac{\partial\widetilde{u}_2}{\partial x_3}-\bigl(k_1^2+k_2^2\bigr)\widetilde{u}_3+(1+\alpha)\dfrac{\partial^2\widetilde{u}_3}{\partial x_3^2}= \\ -\dfrac{F_3}{2\pi\mu}\exp\bigl(ik_1\xi_1+ik_2\xi_2\bigr)\delta(x_3-\xi_3) \end{cases} \tag{4}$$

where $\alpha=1/(1-2\nu)$ is introduced.

The solution of Eq. (4) is $\widetilde{u}_i\sim\exp(s\,x_3)$, where s values should be determined. Substitution into Eq. (4) with $F_i=0$ (homogeneous system) yields the characteristic equation for s:

$$-\bigl(k_1^2+k_2^2-s^2\bigr)^3(1+\alpha)=0. \tag{5}$$

Eq. (5) has thrice degenerated roots $s=\pm k$, where $k=\sqrt{k_1^2+k_2^2}$ is the module of the vector **k**. After the simple, but cumbersome transformations one can find the general homogeneous solution of Eq. (4) as

$$\widetilde{u}_1^h(k_1,k_2,x_3)=\bigl(C_{10}+i\,k_1x_3C_{31}\bigr)\exp(-k\,x_3)+ \\ +\bigl(C_{11}+i\,k_1x_3C_{33}\bigr)\exp(k\,x_3), \tag{6}$$

$$\widetilde{u}_2^h(k_1,k_2,x_3)=\bigl(C_{20}+i\,k_2x_3C_{31}\bigr)\exp(-k\,x_3)+ \\ +\bigl(C_{21}+i\,k_2x_3C_{33}\bigr)\exp(k\,x_3), \tag{7}$$

$$\widetilde{u}_3^h(k_1,k_2,x_3)= \\ =\left(-i\frac{k_1}{k}C_{10}-i\frac{k_2}{k}C_{20}+(3-4\nu)C_{31}+k\,x_3C_{31}\right)\times \\ \times\exp(-k\,x_3)+ \\ +\left(i\frac{k_1}{k}C_{11}+i\frac{k_2}{k}C_{21}+(3-4\nu)C_{33}-k\,x_3C_{33}\right)\exp(k\,x_3). \tag{8}$$

Note, that the equality $1+2/\alpha=3-4\nu$ was used in Eqs. (6)-(8).

To complement the general solution, we seek the particular solution $u_i^p(\mathbf{x})$ of the inhomogeneous Eqs. (4). One of the simplest is the solution for the homogeneous space $u_i^\infty(\mathbf{x})$, since Eq. (1) is reduced to the system of algebraic equations when using the full 3D-Fourier transformation. Its solution has the form:

$$\hat{u}_i^\infty(\mathbf{k})=\hat{G}_{ij}^\infty(\mathbf{k})F_j\exp(i\mathbf{k}\boldsymbol{\xi}),$$

$$\hat{G}_{ij}^\infty(\mathbf{k})=\frac{1}{(2\pi)^{3/2}\mu}\left(\frac{\delta_{ij}}{|\mathbf{k}|^2}-\frac{1}{2(1-\nu)}\frac{k_ik_j}{|\mathbf{k}|^4}\right). \tag{9}$$

The inhomogeneous solution (9) corresponds to the well-known Fourier image of Green's tensor for infinite homogeneous isotropic media (see e.g. Ref. [8]). Looking for solution of the system, confined in x_3-direction, it is convenient to transform (9) to coordinate representation on x_3. Simple integration gives:

$$\widetilde{u}_i^\infty(k_1,k_2,x_3)= \\ =\widetilde{G}_{ij}^\infty(k_1,k_2,x_3-\xi_3)F_j\exp(ik_1\xi_1+ik_2\xi_2), \tag{10}$$

where

$$\widetilde{G}_{11}^\infty(k_1,k_2,x_3-\xi_3)= \\ =\frac{1}{4\pi\mu}\frac{\exp\bigl(-k|x_3-\xi_3|\bigr)}{k}\left(1-\frac{k_1^2\bigl(1+k|x_3-\xi_3|\bigr)}{4(1-\nu)k^2}\right), \tag{11a}$$

$$\widetilde{G}_{12}^\infty(k_1,k_2,x_3-\xi_3)= \\ =-\frac{1}{4\pi\mu}\frac{\exp\bigl(-k|x_3-\xi_3|\bigr)}{k}\frac{k_1k_2\bigl(1+k|x_3-\xi_3|\bigr)}{4(1-\nu)k^2}, \tag{11b}$$

$$\widetilde{G}_{22}^\infty(k_1,k_2,x_3-\xi_3)= \\ =\frac{1}{4\pi\mu}\frac{\exp\bigl(-k|x_3-\xi_3|\bigr)}{k}\left(1-\frac{k_2^2\bigl(1+k|x_3-\xi_3|\bigr)}{4(1-\nu)k^2}\right), \tag{11c}$$

$$\widetilde{G}_{13}^\infty(k_1,k_2,x_3-\xi_3)= \\ =\frac{1}{4\pi\mu}\frac{\exp\bigl(-k|x_3-\xi_3|\bigr)}{k}\frac{i\,k_1(x_3-\xi_3)}{4(1-\nu)}, \tag{11d}$$

$$\widetilde{G}_{23}^\infty(k_1,k_2,x_3-\xi_3)= \\ =\frac{1}{4\pi\mu}\frac{\exp\bigl(-k|x_3-\xi_3|\bigr)}{k}\frac{i\,k_2(x_3-\xi_3)}{4(1-\nu)}, \tag{11e}$$

$$\widetilde{G}_{33}^\infty(k_1,k_2,x_3-\xi_3)= \\ =\frac{1}{4\pi\mu}\frac{\exp\bigl(-k|x_3-\xi_3|\bigr)}{k}\left(1-\frac{1-k|x_3-\xi_3|}{4(1-\nu)}\right), \tag{11f}$$

and $\mu=Y/(2(1+\nu))$.

The general solution of the chosen elastic problem should satisfy the boundary conditions at the rigid substrate is $u_i(x_3=h)=0$ or $u_i(x_3=h)$ and $\sigma_{3i}(x_3=h)$ are continuous for the matched substrate; also $\sigma_{3i}(x_3=0)=0$ at free upper surface. Keeping in mind the Hook law $\sigma_{ij}=c_{ijkl}\,u_{kl}$, where the strain

$u_{kl} = \frac{1}{2}\left(\frac{\partial u_k}{\partial x_l} + \frac{\partial u_l}{\partial x_k}\right)$ and elastic stiffness $c_{ijkl} = \frac{Y}{2(1+\nu)}\left(\frac{2\nu}{1-2\nu}\delta_{ij}\delta_{kl} + \delta_{ik}\delta_{jl} + \delta_{il}\delta_{jk}\right)$, one obtains that: $\sigma_{33} = \frac{Y}{(1+\nu)(1-2\nu)}\left((1-\nu)u_{33} + \nu(u_{11}+u_{22})\right)$, $\sigma_{31} = \frac{Y}{(1+\nu)}u_{13}$, $\sigma_{32} = \frac{Y}{(1+\nu)}u_{23}$.

For the rigid substrate case, the boundary conditions for $\widetilde{u}_i(k_1,k_2,x_3) = \widetilde{u}_i^h(k_1,k_2,x_3) + \widetilde{u}_i^p(k_1,k_2,x_3)$ have the form:

$$\begin{cases} (1-\nu)\dfrac{\partial \widetilde{u}_3}{\partial x_3} - i\nu\left(k_1\widetilde{u}_1 + k_2\widetilde{u}_2\right)\Big|_{x_3=0} = 0, \\ \dfrac{\partial \widetilde{u}_1}{\partial x_3} - ik_1\widetilde{u}_3\Big|_{x_3=0} = 0, \quad \dfrac{\partial \widetilde{u}_2}{\partial x_3} - ik_2\widetilde{u}_3\Big|_{x_3=0} = 0, \\ \widetilde{u}_1\big|_{x_3=h} = 0, \quad \widetilde{u}_2\big|_{x_3=h} = 0, \quad \widetilde{u}_3\big|_{x_3=h} = 0. \end{cases} \tag{12}$$

Six constants C_{ij} should be expressed via F_j from Eqs. (12). For the matched substrate only the first row of Eqs. (12) should be used.

(I) First step. Let us find the Green function $\widetilde{G}_{ij}^s(k_1,k_2,x_3-\xi_3)$ of the semi-space ($h \to \infty$). The function is the solution for the matched substrate case. For the case $C_{11} = C_{21} = C_{33} = 0$ and then Eqs. (12) should be solved allowing for the partial solution $\widetilde{u}_i^p(k_1,k_2,0) \equiv \widetilde{u}_i^\infty(k_1,k_2,0)$. After cumbersome algebraic transformations one derives:

$$\widetilde{u}_i^s(k_1,k_2,x_3) = \widetilde{G}_{ij}^s(k_1,k_2,x_3,\xi_3)F_j\exp(ik_1\xi_1 + ik_2\xi_2). \tag{13}$$

Where

$$\widetilde{G}_{11}^s(k_1,k_2,x_3,\xi_3) = \frac{\exp(-k(x_3+\xi_3))}{16\pi\mu k^3(1-\nu)}\times$$
$$\times\begin{pmatrix} -k_1^2k(x_3+\xi_3)(3-4\nu)+ \\ +2k^2\left(2-2\nu+k_1^2x_3\xi_3\right)+k_1^2\left(1-8(1-\nu)\nu\right)\end{pmatrix}+ \tag{14a}$$
$$+\frac{\exp\left(-k|x_3-\xi_3|\right)}{16\pi\mu k^3(1-\nu)}\left(4k^2(1-\nu)-k_1^2-k_1^2k|x_3-\xi_3|\right),$$

$$\widetilde{G}_{21}^s(k_1,k_2,x_3,\xi_3) = \frac{\exp(-k(x_3+\xi_3))}{16\pi\mu k^3(1-\nu)}\times$$
$$\times k_1k_2\begin{pmatrix} 2k^2x_3\xi_3 - k(x_3+\xi_3)(3-4\nu)+ \\ +1-8(1-\nu)\nu\end{pmatrix}+ \tag{14b}$$
$$+\frac{\exp\left(-k|x_3-\xi_3|\right)}{16\pi\mu k^3(1-\nu)}k_1k_2\left(1+k|x_3-\xi_3|\right),$$

$$\widetilde{G}_{31}^s(k_1,k_2,x_3,\xi_3) = \frac{\exp(-k(x_3+\xi_3))}{16\pi\mu k^2(1-\nu)}ik_1\times$$
$$\times\begin{pmatrix} -2k^2x_3\xi_3 + k(x_3-\xi_3)(3-4\nu)+ \\ +4(1-\nu)(1-2\nu)\end{pmatrix}+ \tag{14c}$$
$$+\frac{\exp(-k|x_3-\xi_3|)}{16\pi\mu k(1-\nu)}ik_1(x_3-\xi_3),$$

$$\widetilde{G}_{12}^s(k_1,k_2,x_3,\xi_3) = \frac{\exp(-k(x_3+\xi_3))}{16\pi\mu k^3(1-\nu)}\times$$
$$k_1k_2\begin{pmatrix} 2k^2x_3\xi_3 - k(x_3+\xi_3)(3-4\nu)+ \\ +1-8(1-\nu)\nu\end{pmatrix}+ \tag{14d}$$
$$+\frac{\exp(-k|x_3-\xi_3|)}{16\pi\mu k^3(1-\nu)}k_1k_2\left(1+k|x_3-\xi_3|\right),$$

$$\widetilde{G}_{22}^s(k_1,k_2,x_3,\xi_3) = \frac{\exp(-k(x_3+\xi_3))}{16\pi\mu k^3(1-\nu)}\times$$
$$\times\begin{pmatrix} -k_2^2k(x_3+\xi_3)(3-4\nu)+ \\ +2k^2\left(2-2\nu+k_2^2x_3\xi_3\right)+k_2^2\left(1-8(1-\nu)\nu\right)\end{pmatrix}+ \tag{14e}$$
$$+\frac{\exp(-k|x_3-\xi_3|)}{16\pi\mu k^3(1-\nu)}\left(4k^2(1-\nu)-k_2^2-k_2^2k|x_3-\xi_3|\right),$$

$$\widetilde{G}_{32}^s(k_1,k_2,x_3,\xi_3) = \frac{\exp(-k(x_3+\xi_3))}{16\pi\mu k^2(1-\nu)}\times$$
$$\times ik_2\begin{pmatrix} -2k^2x_3\xi_3 + k(x_3-\xi_3)(3-4\nu)+ \\ +4(1-\nu)(1-2\nu)\end{pmatrix}+ \tag{14f}$$
$$+\frac{\exp(-k|x_3-\xi_3|)}{16\pi\mu k(1-\nu)}ik_2(x_3-\xi_3),$$

$$\widetilde{G}_{13}^s(k_1,k_2,x_3,\xi_3) = \frac{\exp(-k(x_3+\xi_3))}{16\pi\mu k^2(1-\nu)}\times$$
$$\times ik_1\begin{pmatrix} 2k^2x_3\xi_3 + k(x_3-\xi_3)(3-4\nu)+ \\ -4(1-\nu)(1-2\nu)\end{pmatrix}+ \tag{14g}$$
$$+\frac{\exp(-k|x_3-\xi_3|)}{16\pi\mu k(1-\nu)}ik_1(x_3-\xi_3),$$

$$\widetilde{G}_{23}^s(k_1,k_2,x_3,\xi_3) = \frac{\exp(-k(x_3+\xi_3))}{16\pi\mu k^2(1-\nu)}\times$$
$$\times ik_2\begin{pmatrix} 2k^2x_3\xi_3 + k(x_3-\xi_3)(3-4\nu)- \\ -4(1-\nu)(1-2\nu)\end{pmatrix}+ \tag{14h}$$
$$+\frac{\exp(-k|x_3-\xi_3|)}{16\pi\mu k(1-\nu)}ik_2(x_3-\xi_3),$$

$$\widetilde{G}_{33}^s(k_1,k_2,x_3,\xi_3) = \frac{\exp(-k(x_3+\xi_3))}{16\pi\mu k(1-\nu)}\times$$
$$\times\begin{pmatrix} 2k^2x_3\xi_3 + k(x_3+\xi_3)(3-4\nu)+ \\ +1+4(1-\nu)(1-2\nu)\end{pmatrix}+ \tag{14i}$$
$$+\frac{\exp(-k|x_3-\xi_3|)}{16\pi\mu k(1-\nu)}(3-4\nu+k|x_3-\xi_3|).$$

where $k = \sqrt{k_1^2 + k_2^2}$. Note that

$\widetilde{G}^s_{21}(k_1,k_2,x_3,\xi_3) = \widetilde{G}^s_{12}(k_1,k_2,x_3,\xi_3)$,

$\widetilde{G}^s_{22}(k_1,k_2,x_3,\xi_3) = \widetilde{G}^s_{11}(k_2,k_1,x_3,\xi_3)$,

$\widetilde{G}^s_{32}(k_1,k_2,x_3,\xi_3) = \widetilde{G}^s_{31}(k_2,k_1,x_3,\xi_3)$ as expected.

(II) Second step. Using Eq. (14) as the partial solution $\widetilde{u}_i^p(k_1,k_2,x_3) = \widetilde{u}_i^s(k_1,k_2,x_3)$, let us find the surface vertical displacement $\widetilde{u}_3^f(k_1,k_2,0) = \widetilde{u}_3^h(k_1,k_2,0) + \widetilde{u}_3^s(k_1,k_2,0)$ for the film of the thickness h. Here $\widetilde{u}_3^h(k_1,k_2,0)$ should be found from Eqs. (12), namely after cumbersome algebraic transformations we derived that

$$\widetilde{u}_3^f(k_1,k_2,0) = \widetilde{G}^f_{3j}(k_1,k_2,\xi_3) F_j \exp(ik_1\xi_1 + ik_2\xi_2). \quad (15)$$

Where the elastic Green function $\widetilde{G}^f_{3j}(k_1,k_2,\xi_3)$ for the film on a rigid substrate has the form:

$$\widetilde{G}^f_{3j}(k_1,k_2,\xi_3) = \left(\begin{array}{l} \widetilde{G}^s_{3j}(k_1,k_2,0,\xi_3) - \widetilde{G}^s_{3j}(k_1,k_2,h,\xi_3)\phi_3(k\,h,\nu) + \\ + i\left(k_1\widetilde{G}^s_{1j}(k_1,k_2,h,\xi_3) + k_2\widetilde{G}^s_{2j}(k_1,k_2,h,\xi_3)\right)\phi_\perp(k\,h,\nu) \end{array} \right), \quad (16)$$

$$\phi_3(k\,h,\nu) = \frac{4(1-\nu)(\exp(-k\,h)(2-2\nu-k\,h)+\exp(k\,h)(2-2\nu+k\,h))}{(3-4\nu)(\exp(-2k\,h)+\exp(2k\,h))+2(1+4(1-\nu)(1-2\nu)+2k^2h^2)}, \quad (17a)$$

$$\phi_\perp(k\,h,\nu) = \frac{4(1-\nu)(\exp(-k\,h)(1-2\nu+k\,h)-\exp(k\,h)(1-2\nu-k\,h))}{k\left((3-4\nu)(\exp(-2k\,h)+\exp(2k\,h))+2(1+4(1-\nu)(1-2\nu)+2k^2h^2)\right)}. \quad (17b)$$

Here $k \equiv \sqrt{k_1^2 + k_2^2}$, ν is the Poisson ratio. Note that $\widetilde{G}^f_{3j}(k_1,k_2,0<\xi_3<h) = 0$ at $h = 0$ as it should be expected. For the film on the matched substrate $\phi_3(k\,h,\nu) = 0$ and $\phi_\perp(k\,h,\nu) = 0$.

3. Resolution function and electric field calculations for thin piezoelectric films

The phenomenological resolution function theory for PFM based on linear imaging theory has been introduced in Ref. [9], where the resolution function and the effect of lock-in on resolution have been determined experimentally, and later on theoretically considered in Ref. [5] for the semi-infinite case.

Let us consider the case when the film dielectric and piezoelectric properties differ from bulk or substrate ones. In this case, the strain piezoelectric coefficient $d_{klj}(x_1,x_2,x_3)$ is dependent on the depth x_3 as follows:

$$d_{klj}(x_1,x_2,x_3) = \begin{cases} d^S_{ijk}(x_1,x_2), & 0 \le x_3 \le h \\ 0, & h < x_3 < \infty \end{cases} \quad (18)$$

Here, $d^S_{ijk}(x_1,x_2)$ are the film piezoelectric effect tensor components.

The surface piezoresponse below the tip ($x_3 = 0$) is given by the convolution of piezoelectric coefficients d_{klj} with the surface and bulk components of the resolution function [9]:

$$u_i^S(x_1,x_2,0) = \int_{-\infty}^{\infty} d\xi_1 \int_{-\infty}^{\infty} d\xi_2\, W^f_{ijkl}(\xi_1,\xi_2) d^S_{lkj}(x_1-\xi_1, x_2-\xi_2). \quad (19)$$

The film resolution function [6] components W^f_{ijkl} are introduced as

$$W^f_{ijkl}(\xi_1,\xi_2) = \int_0^h d\xi_3 c_{kjmn} \frac{\partial G^f_{im}(-\xi_1,-\xi_2,\xi_3)}{\partial \xi_n} E_l(\xi_1,\xi_2,\xi_3). \quad (20)$$

$E_k(\mathbf{x})$ is the *ac* electric field distribution produced by the probe.

Hereinafter the effective point charge model [10, 11] is used for electric fields description in the immediate vicinity of the tip-surface junction. Within the framework of the model, the charge value Q and its surface separation d are selected so that corresponding isopotential surface reproduces the tip radius of curvature in the contact point R_0 (or contact radius for flattened tip) and potential U (see Fig. 1). For piezoresponse modeling, the electric field structure can be represented by the point charge model in which the effective charge value Q is equal to the product of tip capacitance $C_t(h)$ on applied voltage $Q(h) = C_t(h)U$.

The electric field potentials $\varphi_{e,i,b}(\mathbf{r})$ created by the point charge Q localized in ambient in the point $r_0 = (0,0,-d)$ outside the layer (film) $0 \le x_3 \le h$ filled by transversely isotropic dielectric with $\varepsilon_{11} = \varepsilon_{22} \ne \varepsilon_{33}$ could be found from the boundary problem:

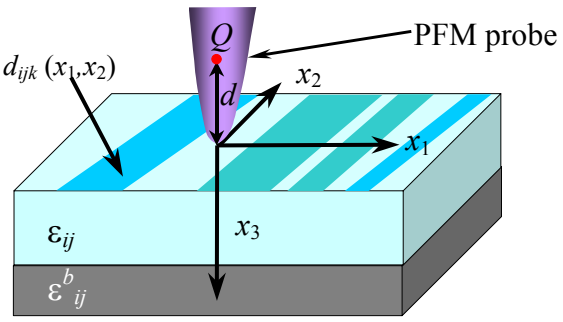

Fig. 1. Point charge model of the PFM probe and scheme of measurements.

$$\Delta\varphi_e(\mathbf{r}) = -\frac{Q}{\varepsilon_0\varepsilon_e}\delta(x_1, x_2, x_3 + d), \qquad x_3 \le 0,$$

$$\varepsilon_{11}\Delta_\perp\varphi_i(\mathbf{r}) + \varepsilon_{33}\frac{\partial^2\varphi_i}{\partial x_3^2} = 0, \qquad 0 \le x_3 \le h,$$

$$\varepsilon_{11}^b\Delta_\perp\varphi_b(\mathbf{r}) + \varepsilon_{33}^b\frac{\partial^2\varphi_b}{\partial x_3^2} = 0, \qquad x_3 \ge h,$$

$$\varphi_e(x_3 = 0) = \varphi_i(x_3 = 0),\ \left(\varepsilon_e\frac{\partial\varphi_e}{\partial x_3} - \varepsilon_{33}\frac{\partial\varphi_i}{\partial x_3}\right)\Bigg|_{x_3=0} = 0,$$

$$\varphi_i(x_3 = h) = \varphi_b(x_3 = h),\ \left(\varepsilon_{33}^b\frac{\partial\varphi_b}{\partial x_3} - \varepsilon_{33}\frac{\partial\varphi_i}{\partial x_3}\right)\Bigg|_{x_3=h} = 0. \tag{21}$$

Note, that $\varphi_i(x_3 = h) = 0$ for a conductive substrate. The solution of Eq. (21) can be found with the help of Hankel integral transformation. Inside the film $0 \le x_3 \le h$, the Fourier representation of the electric field $\widetilde{E}_j(k_1, k_2, x_3)$ acquires the form

$$\widetilde{E}_{1,2}(k_1, k_2, x_3) = ik_{1,2}\frac{Q}{2\pi\varepsilon_0}\times$$
$$\times\frac{(\kappa_b + \kappa)\exp\left(-kd - k\frac{x_3}{\gamma}\right) - (\kappa_b - \kappa)\exp\left(-kd - k\frac{2h - x_3}{\gamma}\right)}{k\left((\kappa_b + \kappa)(\varepsilon_e + \kappa) - (\kappa_b - \kappa)(\varepsilon_e - \kappa)\exp\left(-\frac{2h}{\gamma}k\right)\right)},$$

$$\widetilde{E}_3(k_1, k_2, x_3) = \frac{Q}{2\pi\varepsilon_0}\times$$
$$\times\frac{(\kappa_b + \kappa)\exp\left(-kd - k\frac{x_3}{\gamma}\right) + (\kappa_b - \kappa)\exp\left(-kd - k\frac{2h - x_3}{\gamma}\right)}{\gamma\left((\kappa_b + \kappa)(\varepsilon_e + \kappa) - (\kappa_b - \kappa)(\varepsilon_e - \kappa)\exp\left(-\frac{2h}{\gamma}k\right)\right)}. \tag{22}$$

Here ε_e is the dielectric constant of the ambient, $\kappa = \sqrt{\varepsilon_{33}\varepsilon_{11}}$ is effective dielectric constant, $\gamma = \sqrt{\varepsilon_{33}/\varepsilon_{11}}$ is the dielectric anisotropy factor of the film, $\kappa_b = \sqrt{\varepsilon_{33}^b\varepsilon_{11}^b}$ is effective dielectric constant of the substrate; $-d$ is x_3-coordinate of the effective point charge Q. Usually $d \sim 1 - 100$ nm.

For the conductive disk of radius R_0 representing flattened tip-surface contact area, the effective charge $Q(h) = C_t^{\text{disk}}(h)U$. Calculations performed in Ref. [6] lead to the probe tip effective capacity $C_t^{\text{disk}}(h) \approx 4\varepsilon_0(\varepsilon_e + \kappa)R_0/\psi(h, d)$, where the function

$$\psi(h, d) = \left(\sum_{n=0}^{\infty}\chi^n\left(\frac{\gamma d}{\gamma d + 2hn} - \frac{\kappa_b - \kappa}{\kappa_b + \kappa}\frac{\gamma d}{\gamma d + 2h(n+1)}\right)\right)^{-1}$$

and the parameter $\chi = \left(\frac{\kappa_b - \kappa}{\kappa_b + \kappa}\right)\left(\frac{\varepsilon_e - \kappa}{\varepsilon_e + \kappa}\right)$. The corresponding effective distance $d = 2R_0/\pi$, i.e. d is almost independent on the film thickness h.

For the spherical tip with curvature R_0 in point contact with film surface, the effective charge $Q(h) = C_t^{\text{sph}}(h)U$. We obtained the probe tip capacity

$$C_t^{\text{sph}}(h) \approx 4\pi\varepsilon_0\varepsilon_e R_0\frac{\kappa + \varepsilon_e}{\kappa - \varepsilon_e}\ln\left(\frac{\varepsilon_e + \kappa}{2\varepsilon_e}\right)\times$$
$$\times\left(1 + \frac{\gamma R_0}{h}\frac{2\varepsilon_e\kappa\ln(1-\chi)}{(\varepsilon_e - \kappa)^2}\ln\left(\frac{\varepsilon_e + \kappa}{2\varepsilon_e}\right)\right)$$

and effective distance $d \approx 2\varepsilon_e R_0 \times$ $\times\ln\left((\varepsilon_e + \kappa)/2\varepsilon_e\right)/(\kappa - \varepsilon_e)$ for the film thickness $h \ge 0.1\gamma R_0$ in the actual range of high dielectric constants $\kappa_b, \kappa >> 1$ and $1 \le \varepsilon_e \le 80$ [6].

For the case when the considered surface piezoelectric layer is inhomogeneous in the transverse directions $\{x_1, x_2\}$ (e.g. it is divided into polar regions or posses domain structure with different piezoelectric tensor values and signs $d_{ijk}^S(x_1, x_2)$), the resolution function components W_{ijk}^f allow approximate calculation of the piezoresponse from those structures, which Fourier image $\widetilde{d}_{ijk}^S(\mathbf{q})$ exists in usual (e.g. domain stripes, rings *etc*.) or generalized (infinite plane domain wall) sense. Being more rigorous, one should use the Fourier image of tensorial *object transfer function* components $\widetilde{W}_{ijk}^f(q)$, since the Fourier transform of film vertical piezoresponse $\widetilde{d}_{33}^{\text{eff}}(\mathbf{q})$ over transverse coordinates $\{x_1, x_2\}$ is

$$\widetilde{d}_{33}^{\text{eff}}(\mathbf{q}) = \widetilde{W}_{333}^f\widetilde{d}_{33}^S(\mathbf{q}) + \widetilde{W}_{313}^f\widetilde{d}_{31}^S(\mathbf{q}) + \widetilde{W}_{351}^f\widetilde{d}_{15}^S(\mathbf{q}), \tag{23}$$

where $\widetilde{d}_{33}^{\text{eff}}(\mathbf{q}) = \int d_{33}^{\text{eff}}(\mathbf{x})e^{i\mathbf{q}\mathbf{x}}d\mathbf{x}$ is the Fourier transforms of effective vertical piezoresponse $d_{33}^{\text{eff}} = u_3(\mathbf{x} = 0)/U$; the Voight notation is used. Object transfer function component $\widetilde{W}_{3ij}^f(q)$ spectrum dependent on wavenumber absolute value $q = \sqrt{q_1^2 + q_2^2}$ is shown in Fig. 2a-c for various film thicknesses *h*.

In most cases, the component $\widetilde{W}_{333}^f(q)$ corresponding to the piezoelectric constant d_{33} provides the dominant (>50 %) contribution to the overall signal [5]. The two-point resolution $r_{\min}$ in PFM experiments is determined by the inverse halfwidth of $\widetilde{W}_{333}^f(q)$. The dependence of corresponding two-point resolution $r_{\min}$ on *h*/*d* for different values of anisotropy γ is shown in Fig. 2d. It is clear that the information limit increases with the film thickness decrease because of $r_{\min}$ decrease. The dependence of 180º-periodic domain

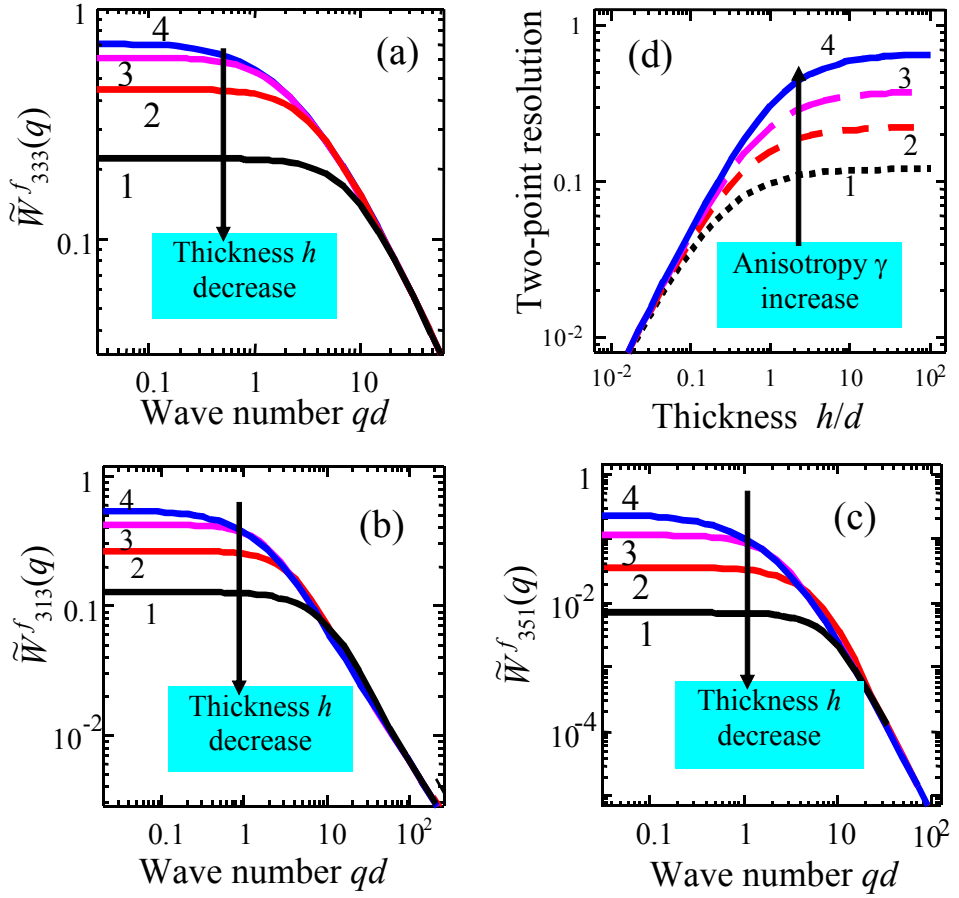

Fig. 2. (a, b, c) Object transfer function components $\widetilde{W}^{f}_{3ij}(q)$ spectrum for anisotropy $\gamma = 1$, permittivity $\kappa = 500$ and relative thickness $h/d = 0.3, 1, 3, 10$ (curves 1, 2, 3, 4); substrate permittivity $\kappa_b = 10$, ambient dielectric constant $\varepsilon_e = 1$. (d) The dependence of corresponding two-point resolution $r_{\min}/d$ on h/d for different values of anisotropy $\gamma = 0.25, 0.5, 1, 3$ (curves 1, 2, 3, 4).

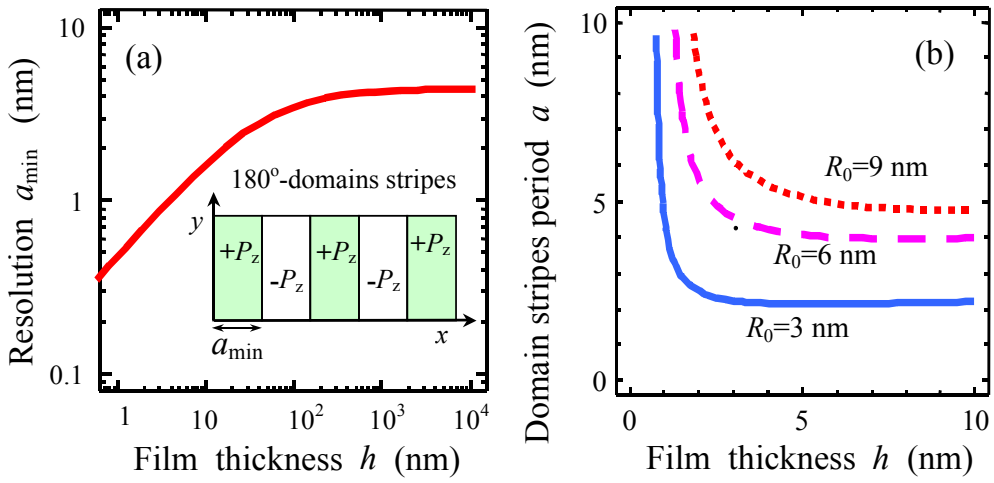

Fig. 3. (a) The dependence of 180°-periodic domain structure resolution $a_{\min}$ via $PbTiO_3$ film thickness h on a rigid substrate for the effective distance $d = 10$ nm. (b) Information limit defined as a minimal domain stripes period a calculated from the condition $\max\left\{d_{33}^{\text{eff}}(a,h)\right\}$ = *noise level* for the $PbTiO_3$ film of the thickness h on a rigid substrate for the typical noise level 1 pm/V and different tip-surface contact radii $R_0 = 3$, 6, 9 nm (effective distance $d = 2R_0/\pi$). (b) $PbTiO_3$ material parameters $\nu = 0.35$, $\kappa = 121$, $\gamma = 0.87$, $d_{33}^S = 117$, $d_{15}^S = 61$, $d_{31}^S = -25$ pm/V, substrate permittivity $\kappa_b = 5$, ambient permittivity $\varepsilon_e = 1$.

structure resolution via the film thickness h and corresponding information limit defined as minimal domain stripes period $a_{\min}$ calculated from the condition $\max\left\{d_{33}^{\text{eff}}(a,h)\right\}$ = *noise level* is shown in Fig. 3 for the $PbTiO_3$ film on a rigid substrate.

4. Conclusion

The elastic Green function and resolution function in Piezoresponse Force Microscopy (PFM) of piezoelectric film capped on the rigid substrate with different dielectric properties are derived.

The thickness dependence of resolution function of the thin piezoelectric films on rigid substrates is demonstrated: minimal lateral resolution (or higher information limit) is possible in thin films. However, the signal amplitude essentially decreases with film thickness decrease, eventually making the noise level relatively higher.

Acknowledgements

Author is grateful to Academician, Prof. S.V. Svechnikov (NAS of Ukraine) and Dr. S.V. Kalinin (Oak Ridge National Laboratory) for valuable remarks.

References

1. *Nanoscale Characterization of Ferroelectric Materials*, ed. M. Alexe and A. Gruverman. Springer, 2004.
2. *Nanoscale Phenomena in Ferroelectric Thin Films*, ed. Seungbum Hong. Kluwer, 2004.
3. F. Felten, G.A. Schneider, J.M. Saldaña, and S.V. Kalinin // *J. Appl. Phys*. **96**, p. 563 (2004).
4. D.A. Scrymgeour and V. Gopalan // *Phys. Rev. B* **72**, 024103 (2005).
5. A.N. Morozovska, E.A. Eliseev, S.L. Bravina, and S.V. Kalinin // *Phys. Rev. B* **75**, 174109-1-18 (2007).
6. A.N. Morozovska, S.V. Svechnikov, E.A. Eliseev, and S.V. Kalinin, Extrinsic size effect in Piezoresponse Force Microscopy of thin films // *Phys. Rev. B* **76**(5), 054123-5 (2007).
7. L.D. Landau and E.M. Lifshitz, *Theory of Elasticity*. *Theoretical Physics, Vol. 7*. Butterworth-Heinemann, Oxford, U.K., 1998.
8. C. Teodosiu, *Elastic Models of Crystal Defects*. Springer-Verlag, Berlin, 1982.
9. S.V. Kalinin, S. Jesse, J. Shin, A.P. Baddorf, H.N. Lee, A. Borisevich, and S.J. Pennycook // *Nanotechnology* **17**, p. 3400 (2006).
10. A.N. Morozovska, E.A. Eliseev, and S.V. Kalinin // *Appl. Phys. Lett.* **89**, 192901 (2006).
11. A.N. Morozovska, S.V. Kalinin, E.A. Eliseev, and S.V. Svechnikov, Local polarization switching in Piezoresponse Force Microscopy // *Ferroelectrics* **354**, p. 198-207 (2007).